PHYSICAL REVIEW E **68**, 065604(R) (2003)

Vectorial Swift-Hohenberg equation for transverse laser patterns

Miguel Hoyuelos and Matías dell'Erba
Departamento de Física, Facultad de Ciencias Exactas y Naturales, Universidad Nacional de Mar del Plata, Funes 3350, 7600 Mar del Plata, Argentina

(Received 16 April 2003; published 17 December 2003)

The consequences of introducing the polarization degree of freedom of the light are studied for the transverse patterns of a laser with detuning equal to zero. We deduce the vectorial Swift-Hohenberg amplitude equation from the corresponding Maxwell-Bloch equations. The vectorial character of the equation introduces modifications in the stability of traveling waves and new types of localized structures.

DOI: 10.1103/PhysRevE.68.065604 PACS number(s): 42.65.Sf, 05.45.Yv, 89.75.Kd

Studies of optical pattern formation [1] share a number of features with general investigation of structures and instabilities in other physical systems [2]. Nevertheless, there are also specific features of optical systems such as the presence of diffraction instead of diffusion and the vectorial degree of freedom associated with the polarization of the light.

Lasers with large aspect ratio present an excellent opportunity for the study of extended structures in nonlinear optical systems. Much work has been already done both theoretically and experimentally [3]. Dotlike localized structures produced by phase singularities [4] have been experimentally observed in lasers [5] and other optical systems [6].

The Maxwell-Bloch (MB) equations can be used to describe transverse patterns in single longitudinal mode lasers, where the active medium is composed of two level atoms inside a cavity with flat mirrors (one of which is partially reflecting). An important parameter for determining the behavior of the system is the cavity detuning $\Omega=(\omega_{12}-\omega_c)/\gamma_\perp$, where ω_{12} is the atomic frequency, ω_c is the cavity resonance frequency closest to ω_{12}, and $\gamma_\perp$ is the decay rate of polarization. From a linear stability analysis [7] it can be shown that the first wave numbers that become unstable as the laser pump is increased are $k_c=0$ if $\Omega<0$ and $k_c=\pm\sqrt{\Omega/a}$ in one-dimension (1D) (or a ring of minima in 2D) if $\Omega>0$, where a is the strength of diffraction.

The direction of the electric field in laser cavities is usually fixed by Brewster windows. The polarization of the field is linear and fixed in one direction. A model where the electric field and the polarization of the medium are scalar quantities is appropriate in this case. Close to the instability threshold, the MB equations can be reduced to an amplitude equation and the system variables can be expressed in terms of only one complex amplitude. If $\Omega<0$, a complex Ginzburg-Landau equation (CGLE) is obtained. If $\Omega>0$, since there are two modes that become unstable simultaneously in 1D, the description requires two coupled CGLEs. If $\Omega=0$, a complex Swift-Hohenberg equation (CSHE) is obtained instead of a CGLE. It has been shown that even for $\Omega\neq 0$, but close to 0, a CSHE is appropriate for the description of the system [8]. Despite the peculiarities of different lasers, an analysis and classification of possible states close to threshold is provided by this equation, at least for class *A* and *C* lasers. (The classification of lasers is based on the relations among the decay rate of population difference $\gamma_\parallel$, the cavity decay rate κ, and $\gamma_\perp$. For a class *A* laser, $\gamma_\perp$, $\gamma_\parallel \gg \kappa$; for a class *B* laser, $\gamma_\perp \gg \kappa \gg \gamma_\parallel$; and for a class *C* laser, $\kappa\sim\gamma_\perp\sim\gamma_\parallel$ [9]. An argument against the validity of the equation for a class *B* laser is provided in Ref. [8].) The CSHE has been used also for the description of optical parametric oscillators [10] and photorefractive materials, where it has qualitatively reproduced experimental results [11].

In this paper we will focus on the laser MB equations for the case $\Omega=0$, and will generalize the results for the situation when the polarization degree of freedom is taken into account (for example, by removing the Brewster windows). We consider as a prototype situation, transitions from states $J_z=\pm 1$ in the upper level to $J=0$ in the lower level, which produces the circularly polarized components of the electric field. The standard MB equations are extended to [12,13],

$$\frac{\partial E_\pm}{\partial t}=ia\nabla^2 E_\pm-\sigma E_\pm+\sigma P_\pm,$$

$$\frac{\partial P_+}{\partial t}=-(1+i\Omega)P_+ + rE_+ - N_+E_+ - ME_-,$$

$$\frac{\partial P_-}{\partial t}=-(1+i\Omega)P_- + rE_- - N_-E_- - M^*E_+,$$

$$\frac{\partial N_\pm}{\partial t}=-bN_\pm+\frac{1}{2}(E_\pm^* P_\pm + E_\pm P_\pm^*)+\frac{1}{4}(E_\mp^* P_\mp + E_\mp P_\mp^*),$$

$$\frac{\partial M}{\partial t}=-cM+\frac{1}{4}(E_+P_-^*+E_-^*P_+), \tag{1}$$

where $E_\pm=(E_x\pm iE_y)/\sqrt{2}$ are the right and left circularly polarized components of the electric field, $P_\pm$ are the complex material polarizations, $N_\pm$ are the population differences between levels $(J=1,J_z=\pm 1)$ and $(J=0)$, and M describes interaction between upper level states $(J_z=1)$ and $(J_z=-1)$. The parameters are $a=c_l^2/(2\omega_c\gamma_\perp)$, the strength of diffraction, where c_l is the speed of light; r is proportional to the pumping and plays the role of control parameter; σ, b, and c are normalized material decay rates, particularly $\sigma=\kappa/\gamma_\perp$ and $b=\gamma_\parallel/\gamma_\perp$. The time is adimensional and is scaled with $\gamma_\perp$. $\nabla^2=\partial_x^2+\partial_y^2$ is the Laplacian in the plane perpendicular to light propagation. The fast variation, $\exp(ik_z z-i\omega_c t)$, has been eliminated using the slowly varying

envelope approximation. Equations (1) have been studied in the case $\Omega<0$, where via the reductive perturbation method a vector CGLE is obtained [13].

The nonlasing state ($E_\pm=P_\pm=N_\pm=M=0$) becomes unstable if the control parameter r is greater than a critical value r_c, with $r_c=1$ for $\Omega=0$. It can be shown that, above threshold, the modes that grow are the ones that have wave numbers k within a band of width $R^{1/4}$ centered about $k_c=0$, where $R=r-1$ is the distance to threshold. The appropriate scaling for the spatial variables is $X=R^{1/4}x$ and $Y=R^{1/4}y$. The real and imaginary parts of the eigenvalue of the active mode have different slow time scales, namely, $T_1=R^{1/2}t$ and $T_2=Rt$. Introducing these changes of variables in Eqs. (1), identifying coefficients of different orders of R, and applying the solvability condition, we obtain the vectorial Swift-Hohenberg equation,

$$(1+\sigma)\frac{\partial A_\pm}{\partial t}=\sigma R A_\pm+ia\nabla^2 A_\pm-\frac{\sigma a^2}{(1+\sigma)^2}\nabla^4 A_\pm-\frac{\sigma R}{b}\left(|A_\pm|^2+\frac{b+c}{2c}|A_\mp|^2\right)A_\pm, \qquad (2)$$

where we have returned to the original space and time scales. The interest in amplitude equations such as Eq. (2) resides in their universality. Many physical systems with the same kind of instability and same symmetries can be described with the same equation; and the fact that, close to threshold, all the system variables are equal to the amplitude $A_\pm$ times the unstable eigenvector. For example, the electric field components are $E_\pm=R^{1/2}A_\pm$ [14]. The number of free parameters of Eq. (2) can be reduced using the following scaling: $x\to x(2\sigma a)^{1/2}/(1+\sigma)$, $t\to t\,4\sigma/(1+\sigma)$, $A_\pm\to A_\pm(1+\sigma)b^{1/2}/(2\sigma R^{1/2})$. The resulting equation is,

$$\frac{\partial A_\pm}{\partial t}=(\epsilon-1)A_\pm+(1+i\nabla^2)^2A_\pm-(|A_\pm|^2+\gamma|A_\mp|^2)A_\pm, \qquad (3)$$

where $\epsilon=R\,4\sigma^2/(1+\sigma)^2$ is proportional to the distance to threshold, and the coupling parameter γ is related to material decay rates [$\gamma=(b+c)/(2c)$]. The main difference with the form of the standard Swift-Hohenberg equation is that the Laplacian is imaginary, representing diffraction instead of diffusion; this difference makes the usual potential [2] not suitable in this case. Equation (3) is a simple model, with only two free parameters, useful to theoretically study transverse patterns in lasers at peak gain ($\Omega=0$) and when the vectorial degree of freedom of the light is taken into account. (It can be shown that the necessary precision for the condition $\Omega=0$ is $\Omega\ll R$.) Since b and c are positive constants and $c>b$, the range of possible values of γ is between 1/2 and 1. But, as we mentioned before, one of the main qualities of amplitude equations is their universality. Then, because of the potential application of Eq. (3) to other physical systems (mainly optical) it is interesting to study its behavior for all possible values of parameters ϵ and γ.

The homogeneous stationary solutions coincide with the ones that are obtained for the vector CGLE with real coefficients [15]. A more general solution is a family of traveling waves in 1D,

$$A_\pm=Q_\pm e^{i(k_\pm x-\omega_\pm t+\theta_{0\pm})}, \qquad (4)$$

where $Q_\pm^2+\gamma Q_\mp^2=\epsilon-k_\pm^4$ and $\omega_\pm=2k_\pm^2$. We will consider the situation where both amplitudes Q_+ and Q_- are different from zero. This is the case when $-1<\gamma<1$. Due to the symmetric intensity coupling of Eq. (3), both amplitudes tend to the same value, $Q_+=Q_-=Q$. So, $|k_+|=|k_-|=k$ and $\omega_+=\omega_-=\omega$. We have $Q^2=(\epsilon-k^4)/(1+\gamma)$ and $\omega=2k^2$. There is a range of possible values of the wave number, $0<k<\epsilon^{1/4}$, and there are two possible cases: copropagating waves ($k_+=k_-$) and counterpropagating waves or standing wave ($k_+=-k_-$). We investigate the stability of these two cases (submitted to long-wavelength perturbations corresponding to Eckhaus instability) and summarize the results by drawing the domains of existence and stability in the (ϵ,k) plane (Busse balloon).

For copropagating waves ($k_+=k_-$), after the adiabatic elimination of the amplitude equations, the phase equations turn out to be decoupled,

$$\partial_t\phi_\pm=-4k\partial_x\phi_\pm+\left(6k^2-\frac{8k^6}{Q^2(1\pm\gamma)}\right)\partial^2\phi_\pm, \qquad (5)$$

where $\phi_\pm=\theta_+\pm\theta_-$, with $\theta_\pm$ being the phase perturbation of the solution (4); ϕ_+ is the global phase and ϕ_- is the relative phase associated with a polarization instability. The stability condition associated to the global phase is $\epsilon>(7/3)k^4$, which is equal to the one obtained for the scalar case. The vectorial degree of freedom adds a new stability condition, given by $\epsilon>k^4(7+\gamma)/[3(1-\gamma)]$, which corresponds to the relative phase; this condition is more restrictive than the previous one for $0<\gamma<1$.

For counterpropagating waves ($k_+=-k_-$), coupled phase equations are obtained,

$$\partial_t\phi_\pm=-4k\partial_x\phi_\mp+\left(6k^2-\frac{8k^6}{Q^2(1\mp\gamma)}\right)\partial^2\phi_\pm. \qquad (6)$$

Equation (6) has two equal stability conditions, namely, $\epsilon>k^4(7-3\gamma)/[3(1-\gamma)]$. This condition is, again, more restrictive than the one that corresponds to the scalar case for $0<\gamma<1$.

In Fig. 1 we show the stability regions for both cases. Note that, when $\gamma\to0$, the stability conditions tend to $\epsilon>7/3k^4$ (scalar case), since, in this case, the vectorial Eq. (3) is transformed into two independent scalar equations. When $\gamma\to1$ from the left, the Busse balloon shrinks to a narrow vertical band centered about $k=0$. The stability domain disappears for $\gamma>1$ and traveling waves with equal amplitude in both fields are no longer stable.

The main result of the previous linear stability analysis is that the vectorial case is not a trivial extension of the scalar case, since drastic changes in the stability of traveling waves are introduced.

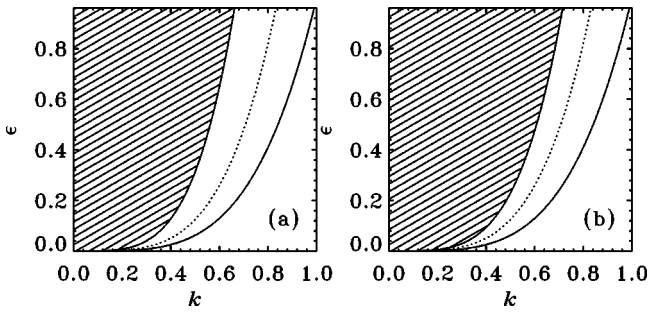

FIG. 1. Existence and stability regions of the traveling wave solution. The continuous line is the limit of the existence domain. The dotted line is the limit of the stability domain in the scalar case (or $\gamma=0$). The region filled with parallel lines is the stability domain of traveling waves with $\gamma=0.5$. (a) Copropagating waves, (b) counterpropagating waves.

Starting from random initial conditions in 2D, we found numerically [16] a rich variety of behaviors. We mention only three characteristic situations, shown in Fig. 2. In Figs. 2(a) and 2(b) we show amplitude and phase of one of the components of the field for $\epsilon=0.3$ and $\gamma=0.1$; domains with a phase singularity delimited by shock waves are seen in the amplitude, while spiral patterns appear in the phase. Similar patterns have been found in the scalar [17,18] or vectorial CGLE [19,15]; the difference here is that the spirals appear distorted, with great variations of the pitch. The amplitude evolves very slowly in time; this situation is usually considered as a frozen phase [20]. Patterns obtained for the parameters in the allowable range for lasers are of this kind. Figures 2(c) and 2(d) corresponds to $\epsilon=1.5$ and $\gamma=1.5$; for $\gamma>1$ the homogeneous stable solutions are $Q_{\pm}=0$, $Q_{\mp}^2=\epsilon$, and the system segregates in regions where each solution dominates. There are also defects or phase singularities. The bright dots in black background correspond to defects in the other component of the field. Note that, in this case, the phase spirals are two armed, meaning that the topological charge of the defects is $n=\pm 2$. This is not a common situation since usually defects with topological charge $|n|>1$ are unstable and detach in defects of smaller charge. Figures 2(e) and 2(f) correspond to $\epsilon=2$ and $\gamma=0.1$; in this case, the defect-dominated pattern gives place to a plane wave. The role of the defects is reduced to dislocations in the stripe pattern, as is clearly seen in the phase plot [Fig. 2(f)]. The defects are drifted in the direction of propagation of the plane wave. In some cases, the defects arrange in stable and complex structures as the one shown in Fig. 3. The structure moves as a rigid body in the direction of the arrow.

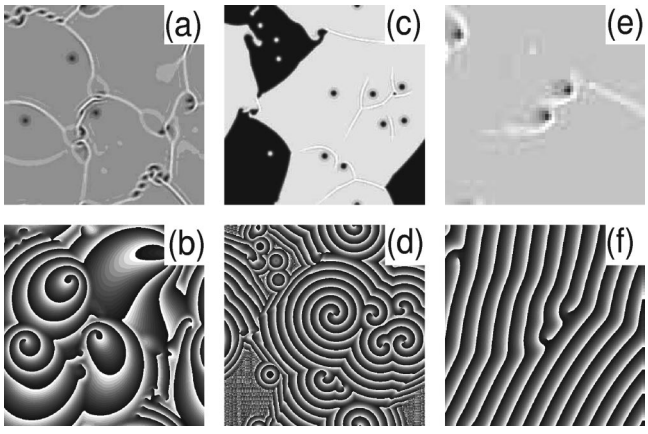

FIG. 2. Numerical results starting from random initial conditions. Top row: $|A_+|$, bottom row: phase θ_+. (a) and (b) $\epsilon=0.3$, $\gamma=0.1$; (c) and (d) $\epsilon=1.5$, $\gamma=1.5$; (e) and (f) $\epsilon=2$, $\gamma=0.1$.

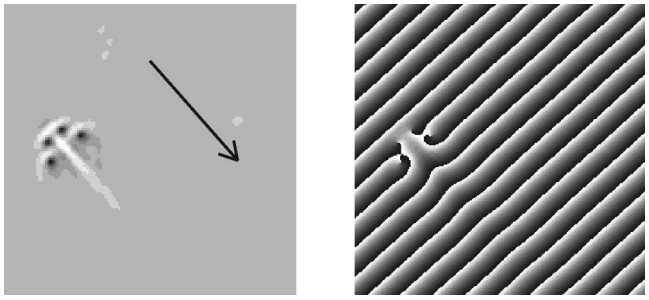

FIG. 3. Rigid and symmetric structure of defects that move in the direction of the arrow. From left to right, amplitude $|A_+|$ and phase θ_+. Parameters: $\epsilon=2$, $\gamma=0.1$.

We found that, for some specific values of the parameters (for example, $\epsilon=1$ and $\gamma=-0.1$), vectorial topological defects are stable (see Fig. 4). These are defects that are present simultaneously in both components of the field at the same point [21,22].

Another interesting and new localized structure is an amplitude spiral (note that, in optical pattern formation, spirals usually appear only in the phase) shown in Fig. 5. The figure shows that the amplitude spiral is directly related with the module of the phase gradient. Another important factor for the formation of this structure is the presence of the vectorial coupling between the components of the field. The amplitude spiral disappears if the coupling is eliminated.

In conclusion, we introduced the vectorial CSHE for the description of transverse patterns of lasers at peak gain. The

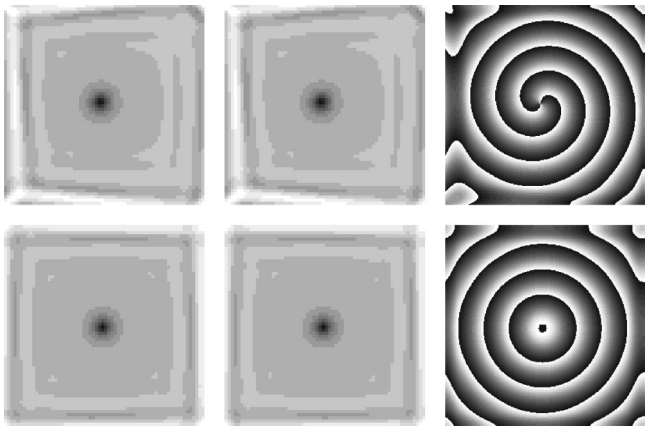

FIG. 4. Vectorial defects. From left to right, $|A_+|$, $|A_-|$ and global phase $\phi_+=\theta_++\theta_-$. Top row: argument defect (same charge). Bottom row: director defect (opposite charge). A two-armed spiral appears in the global phase of the argument defect while a target pattern appears for the director defect. Parameters: $\epsilon=1$, $\gamma=-0.1$.

FIG. 5. From left to right, $|A_+|$ (black=0.9,white=1.05), θ_+, and $|\nabla\theta_+|$. The amplitude spiral is directly related with the gradient of the phase. Parameters: $\epsilon=0.5$, $\gamma=-0.5$.

vectorial character of the equation modifies the stability of traveling waves via a polarization instability. Numerical simulations reveal a wide variety of behaviors and localized structures. Some of them were already seen in other amplitude equation models, such as vectorial defects, domains separated by shock waves, and segregation and competition between two different homogeneous solutions. Others were not previously reported in optical systems, such as spiral waves with distorted pitch, phase singularities with charge greater than 1, and amplitude spirals, which require further and more extensive analysis.

M.H. thanks M. San Miguel, E. Hernández-García, P. Colet, and G. Izús for helpful discussions. This work was partially supported by Consejo Nacional de Investigaciones Científicas y Técnicas (CONICET, Argentina, Grant No. PIP 4342/96) and Agencia Nacional de Promoción Científica y Tecnológica (ANPCyT, Argentina, Grant No. PICTO 2000-2001, Grant No. 03-08431).

[1] *Nonlinear Dynamics in Optical Systems*, edited by N.B. Abraham, E. Garmire, and P. Mandel (Optical Society of America, Washington D.C., 1991); *Nonlinear Optical Structures, Patterns, Chaos*, edited by L.A. Lugiato, special issue of Chaos, Solitons and Fractals **4** 1251 (1994); L.A. Lugiato, M. Brambilla, and A. Gatti, Adv. At., Mol., Opt. Phys. **40**, 229 (1999).

[2] M.C. Cross and P.C. Hohenberg, Rev. Mod. Phys. **65**, 851 (1993).

[3] J.R. Tredicce, E.J. Quel, A.M. Ghazzawi, C. Green, M.A. Pernigo, L.M. Narducci, and L.A. Lugiato, Phys. Rev. Lett. **62**, 1274 (1989); C. Green, G.B. Mindlin, E.J. D'Angelo, H.G. Solari, and J.R. Tredicce, *ibid.* **65**, 3124 (1990); E.J. D'Angelo, E. Izaguirre, G.B. Mindlin, G. Huyet, L. Gil, and J.R. Tredicce, *ibid.* **68**, 3702 (1992).

[4] H. Riecke, in *Pattern Formation in Continuous and Coupled Systems*, edited by M. Golubitsky, D. Luss and S.H. Strogatz (Springer, New York, 1999); L.M. Pismen, *Vortices in Nonlinear Fields* (Oxford University Press, New York, 1999).

[5] D. Dangoisse, D. Hennequin, C. Lepers, E. Louvergneaux, and P. Glorieux, Phys. Rev. A **46**, 5955 (1992); N.R. Heckenberg *et al.*, Opt. Quantum Electron. **24**, S951 (1992).

[6] F.T. Arecchi, G. Giacomelli, P.L. Ramazza, and S. Residori, Phys. Rev. Lett. **67**, 3749 (1991); G. Indebetouw, J. Mod. Opt. **40**, 73 (1993).

[7] A.C. Newell and J.V. Moloney, *Nonlinear Optics* (Addison-Wesley, Redwood City, CA, 1992).

[8] J. Lega, J.V. Moloney, and A.C. Newell, Phys. Rev. Lett. **73**, 2978 (1994).

[9] L.M. Narducci and N.B. Abraham, *Laser Physics and Laser Instabilities* (World Scientific, Singapore, 1988).

[10] M. Santagiustina, E. Hernández-García, M. San-Miguel, A.J. Scroggie, and G.-L. Oppo, Phys. Rev. E **65**, 036610 (2002). (See Appendix II.)

[11] K. Staliūnas, G. Šlekys, and C.O. Weiss, Phys. Rev. Lett. **79**, 2658 (1997).

[12] M. San Miguel, Q. Feng, J.V. Moloney, and A.C. Newell, in *Fluctuation Phenomena: Disorder and Nonlinearity*, edited by A. Bishop, S. Jimenez, and L. Vazquez (World Scientific, Singapore, 1995).

[13] M. San Miguel, Phys. Rev. Lett. **75**, 425 (1995).

[14] The electric field in the MB equations is adimensional. To recover the proper units it has to be multiplied by $\hbar\gamma_\perp/(2p)$, where p is the magnitude of the dipole matrix element $\mathbf{p}_{12}=e\int\mathbf{r}\psi_1^*\psi_2\,d\mathbf{r}$, with ψ_1 and ψ_2 being the wave functions of the lower and upper levels. See Ref. [7].

[15] M. Hoyuelos, E. Hernández-García, P. Colet, and M. San Miguel, Physica D **174**, 176 (2003).

[16] We use a numerical pseudospectral method with second order accuracy in time in lattices of size 128×128 or 256×256. The spatial and temporal discretizations were $\Delta x=1$, and $\Delta t=0.05$. For details, see Ref. [20].

[17] P. Coullet and K. Emilsson, Physica D **61**, 119 (1992).

[18] H. Chaté and P. Manneville, Physica A **224**, 348 (1996).

[19] E. Hernández-García, M. Hoyuelos, P. Colet, and M. San Miguel, Phys. Rev. Lett. **85**, 744 (2000).

[20] M. Hoyuelos, E. Hernández-García, P. Colet, and M. San Miguel, Comput. Phys. Commun. **121**, 414 (1999).

[21] L.M. Pismen, Phys. Rev. Lett. **72**, 2557 (1994); Physica D **73**, 244 (1994).

[22] L. Gil, Phys. Rev. Lett. **70**, 162 (1993).